

# The retinitis pigmentosa protein RP2 links pericentriolar vesicle transport between the Golgi and the primary cilium

R. Jane Evans<sup>1,†</sup>, Nele Schwarz<sup>1,†</sup>, Kerstin Nagel-Wolfrum<sup>2</sup>, Uwe Wolfrum<sup>2</sup>, Alison J. Hardcastle<sup>1</sup> and Michael E. Cheetham<sup>1,\*</sup>

<sup>1</sup>UCL Institute of Ophthalmology, 11-43 Bath Street, London EC1V 9EL, UK and <sup>2</sup>Johannes Gutenberg University of Mainz, Muellerweg 6, 55099 Mainz, Germany

Received December 10, 2009; Revised and Accepted January 11, 2010

**Photoreceptors are complex ciliated sensory neurons. The basal body and periciliary ridge of photoreceptors function in association with the Golgi complex to regulate the export of proteins from the inner segment to the outer segment sensory axoneme. Here, we show that the retinitis pigmentosa protein RP2, which is a GTPase activating protein (GAP) for Arl3, localizes to the ciliary apparatus, namely the basal body and the associated centriole at the base of the photoreceptor cilium. Targeting to the ciliary base was dependent on N-terminal myristoylation. RP2 also localized to the Golgi and periciliary ridge of photoreceptors, which suggested a role for RP2 in regulating vesicle traffic and docking. To explore this hypothesis, we investigated the effect of RP2 depletion and the expression of a constitutively active form of Arl3 (Q71L) on pericentriolar vesicle transport. Kif3a, a component of intraflagellar transport (IFT), is important in cilia maintenance and transport of proteins through the connecting cilium in photoreceptors. Similar to Kif3a and Arl3 depletion, loss of RP2 led to fragmentation of the Golgi network. Depletion of RP2 and dysregulation of Arl3 resulted in dispersal of vesicles cycling cargo from the Golgi complex to the cilium, including the IFT protein IFT20. We propose that RP2 regulation of Arl3 is important for maintaining Golgi cohesion, facilitating the transport and docking of vesicles and thereby carrying proteins to the base of the photoreceptor connecting cilium for transport to the outer segment.**

## INTRODUCTION

Retinitis pigmentosa (RP) defines a clinically and genetically diverse group of retinal dystrophies, which are characterized by progressive photoreceptor cell degeneration. Patients present with night blindness and loss of peripheral vision as the rod photoreceptor cells dysfunction and die, followed by cone photoreceptor cell death. Retinal degeneration progresses towards the central retina, leading to characteristic tunnel vision and eventual blindness.

X-linked RP (XLRP) is the most severe form of RP with mutations in the *RP2* gene accounting for ~15% of all XLRP cases (1–3). Despite the progress that has been made over the years, RP2 function in the retina is unknown. RP2 is a ubiquitously expressed 350 amino acid protein which

does not appear to be enriched in retina (1,4). Dual N-terminal acyl modification by myristoylation and palmitoylation target the protein to the cytoplasmic face of the plasma membrane in cultured cells (4) and in cells throughout the retina (5). Pathogenic mutations at the N-terminus have been shown to prevent plasma membrane localization of RP2 (4,6,7), illustrating that post-translational modifications are vital for correct localization and function of the protein.

To date, the only identified interacting partner of RP2 is the ADP ribosylation factor (Arf)-like protein Arl3 (8). Small GTPases, like Arl3, are regulated by their nucleotide binding. Guanine nucleotide exchange factors (GEFs) stimulate GTP binding that activates signalling through effector proteins, whereas GTPase activating proteins (GAPs) terminate their signalling. RP2 binds the GTP form of Arl3 and was

\*To whom correspondence should be addressed at: Division of Molecular and Cellular Neuroscience, UCL Institute of Ophthalmology, 11-43 Bath Street, London EC1V 9EL, UK. Tel: +44 2076086944; Fax: +44 2076084002; Email:michael.cheetham@ucl.ac.uk

<sup>†</sup>The authors wish it to be known that, in their opinion, the first two authors should be regarded as joint First Authors.

initially thought to be an effector, but detailed structural and biochemical analyses showed that RP2 functions as a GAP for Arl3 (9). Therefore, RP2 is predicted to be a negative regulator of Arl3. Arl3 is a ubiquitous microtubule-associated protein (MAP), which is localized to the connecting cilium in photoreceptors (5). Arl3 knock-out mice have abnormal epithelial cell proliferation and cyst formation in kidney, liver and pancreas, with photoreceptor degeneration in the retina (10). Overall, this phenotype is consistent with a failure of function or signal transduction in primary cilia (11).

Cilia-related disorders (ciliopathies) have been implicated in renal cystic diseases, retinal degeneration, liver fibrosis, anosmia, ataxia, cardiac defects and situs inversus making primary cilia dysfunction the underlying aetiology of numerous genetic disorders (12–16). Many of the genes that cause ciliopathies encode functional or structural components of primary cilia or basal bodies. Mutations in these genes can lead to complete absence or partial loss of cilium expression, or render a morphologically intact cilium dysfunctional (16).

Cilia assembly and maintenance requires coordinated intra-flagellar transport (IFT) of proteins from the basal body along the axoneme to the tip of the cilium. Disruption of this transport mechanism in photoreceptors can lead to cell death and consequently retinal degeneration. For example, knock-down of Kif3a, a subunit of the anterograde IFT motor, results in mislocalization of opsin and photoreceptor cell death (17,18). In addition, mice with mutations in the IFT complex protein IFT88/polaris have abnormal outer segment development and show opsin accumulation in the inner segment and extracellular vesicles (19). Proteins targeted for the primary cilium are trafficked from the Golgi complex to the basal body and to the periciliary ridge in photoreceptors (20). The Golgi complex, periciliary ridge and the basal body complex function in close association with each other to control and regulate export and import from the inner to the outer segment of photoreceptor cells (20). These organelles contain complex protein networks, such as the mammalian Usher proteins, which function as docking sites at the ciliary ridge for vesicles originating from the Golgi network (21). The IFT process is especially sensitive in photoreceptor cells, as the rod outer segment is continuously turned over at a high rate. Changes in protein composition and defects in IFT motor or particle proteins due to mutations lead to retina degeneration (22,23).

RP2 has a region of similarity to the tubulin folding cofactor, cofactor C (TBCC) which was proposed to be essential in tubulin biogenesis (1,24). Many eukaryotes encode several TBCC-like proteins that can be resolved into three distinct clades based on their TBCC domain (25). These clades are defined by the canonical human proteins TBCC, TBCCD1 and RP2. The precise function of these related domains remains unclear, but clues are starting to emerge that their function may be linked to centrioles. For example, a *Trypanosome* protein with the RP2 class of TBCC domain (TbRP2), but no other similarity to human RP2, was linked to flagella function. Ablation of TbRP2 caused shortened flagella and defective axonemal microtubule formation, but had no effect on other microtubule structures or functions including spindle formation. TbRP2 localized to the mature basal body of the flagellum, suggesting flagellum-specific functions

of the protein (25). More recently, a *Chlamydomonas* protein of the TBCCD1 clade (ASQ2) was shown to be required for mother-daughter centriole linkage and mitotic spindle orientation (26). Therefore, a conservation of TBCC family function with centrioles would suggest RP2, in concert with Arl3, might participate in cilia function.

Here, we have investigated the cellular role and localization of RP2 with particular emphasis on understanding its potential role in traffic. In addition to our previously published localization of RP2 at the plasma membrane, a pool of RP2 specifically localizes to the basal body, the Golgi complex and the periciliary ridge of photoreceptors. These organelles function in close association to control export from the outer segment of photoreceptors. Dysregulation of Arl3, by RP2 siRNA or expression of a constitutively active form of Arl3, resulted in dispersal of vesicles cycling cargo from the Golgi complex to the cilium, including the IFT protein IFT20. Therefore, we propose that RP2 regulation of Arl3 is important for maintaining photoreceptor pericentriolar traffic.

## RESULTS

### RP2 localizes to the basal body

RP2 targeting to the cytoplasmic face of the plasma membrane is mediated by dual acylation (4,5,7). In mouse retina, RP2 was detected on the plasma membrane and in the ciliary region of photoreceptor cells between the inner and outer segment (IS and OS, respectively) (Fig. 1A). RP2 localization to the ciliary apparatus in the cilium associated centriole and the basal body was confirmed by high-resolution imaging of the photoreceptor layer of mouse retina sections, where RP2 co-localized with the centriole/basal body marker centrin-3 (27) in the centriole/basal body region at the base of the photoreceptor connecting cilium (Fig. 1B). Immunoelectron microscopy of mouse retina sections revealed specific RP2 labelling was present in the centriole and in the periphery of the basal body of the photoreceptor cilium, but not the connecting cilium or the apical axoneme (Fig. 1C; Supplementary Material, Fig. S1).

RP2 basal body localization was confirmed for primary cilia of human retina pigment epithelial cells (ARPE19). RP2 localized predominantly on the plasma membrane, but a distinct pool of RP2 co-localized with the centrosomal markers  $\gamma$ -tubulin and pericentrin (Fig. 1D). RP2 staining overlapped with  $\gamma$ -tubulin at the basal body, whereas pericentrin stained the periphery of the basal body encircling RP2. Following treatment of ARPE19 cells with a siRNA specific to RP2, membrane and basal body RP2 staining was reduced to undetectable levels in over 80% of the cells (Fig. 1E and F). The specificity of the RP2 antibody staining was confirmed by pre-absorption (Supplementary Material, Fig. S2).

RP2 siRNA appeared to have no major adverse effect on ARPE19 phenotype. For example, cell survival and division of ARPE19s was comparable to cells treated with control siRNA (data not shown). Stephan *et al.* (25) observed no mitotic defects in *Trypanosomes* lacking TbRP2. However, ablation of TbRP2 resulted in abnormally short flagella and loss of tyrosinated  $\alpha$ -tubulin staining (YL 1/2) at the basal body of the flagella, leading to the proposal that TbRP2

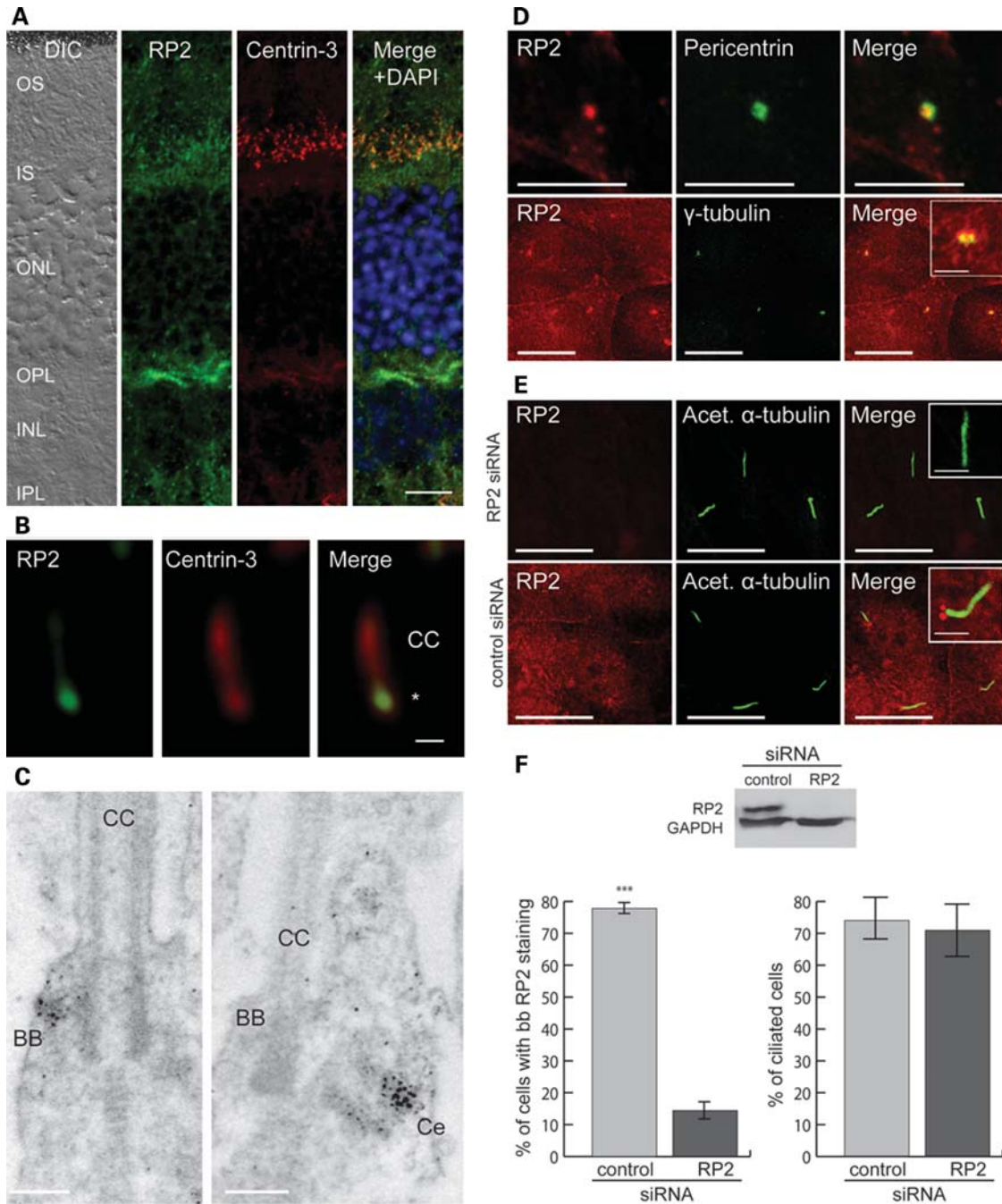


**Figure 1.** RP2 localizes to the basal body. (A) Mouse retina cryosections were stained for endogenous RP2 (green) and counterstained for the ciliary marker centrin-3 (red) and DAPI (blue) nuclear stain for the outer (ONL) and inner nuclear layer (INL). RP2 partially co-localized with centrin-3 in the ciliary region of photoreceptor cells in mouse retina cryosections between the outer segment (OS) and inner segment (IS). RP2 also localized to the synapses between photoreceptors and secondary neurons in the outer plexiform layer (OPL). IPL, inner plexiform layer; DIC, differential interference contrast image. Scale bar 10 μm. (B) Higher magnification of the ciliary region in photoreceptors of the mouse retina. RP2 co-localized with centrin-3 in the centriole/basal body region (asterisk) of photoreceptor cells, but not in the connecting cilium. Scale bar 1 μm. (C) Immunoelectron microscopy of RP2 localization in longitudinal sections through the ciliary apparatus of retinal photoreceptor cells. RP2 labelling in 'basal body satellites' lateral to the basal body (BB) (right image) and in the cilium associated centriole (Ce) (right image, note: 'basal body satellites' are not in the plane of the section). In contrast, the connecting cilium (CC) of photoreceptor cells was RP2 negative. Scale bars 0.2 μm. (D) In human retina pigment epithelial cells (ARPE19), endogenous RP2 (red) co-localized with the basal body marker pericentrin (green), scale bar 5 μm; and γ-tubulin (green), scale bar 10 μm. Inset shows a higher magnification of RP2 basal body localization. Scale bar 2 μm. (E) RP2 localization at the plasma membrane and the basal body was abolished by RP2 specific siRNA, but not with control siRNA. RP2 (red) and the cilia marker acetylated α-tubulin (green). Scale bar 10 μm. Insets show a higher magnification of RP2 basal body localization. Scale bar 2 μm. (F) RP2 localization to the basal body was significantly reduced following RP2 siRNA treatment but there was no effect on the presence of cilia. Experiments were performed in duplicate and in three independent experiments. Values are means ± SEM, n = 300 cells. \*\*\*P ≤ 0.001. Western blotting showed that RP2 siRNA specifically targeted RP2 expression. GAPDH was used to control for equal protein loading.

functions as a quality control protein, assessing the GTPase proficiency of newly formed tubulin heterodimers before incorporation into the flagellum (25). Therefore, we examined cilia length and YL 1/2 staining following RP2 siRNA treatment. The number of cells displaying cilia, cilia morphology and length were unaffected (Fig. 1E and F, Supplementary Material, Fig. S3). In addition, RP2 knock-down did not affect localization of YL 1/2 and basal body markers, such as  $\gamma$ -tubulin, ninein and pericentrin (Supplementary Material, Figs S4 and S5).

### RP2 basal body localization is dependent on protein myristoylation

To determine which domain of the RP2 protein is essential for localization at the ciliary base, IMCD3 cells were transfected with wild-type and mutant RP2 (4). Wild-type RP2 localized to the basal body, whereas basal body localization was lost with the myristoylation mutant (G2AC3S; Fig. 2). Modification of RP2 by palmitoylation requires prior myristoylation. A mutant that targeted the palmitoylation site alone (C3S) localized to the basal body revealing that acylation by myristoylation alone is required for basal body targeting. The patient mutations R118H, which inhibits RP2 GAP activity for Arl3 (9), and L253R, which destabilizes the C-terminal NDK-like domain (9,28), did not affect basal body localization. These data demonstrate that myristoylation is required to target RP2 to the basal body, whereas palmitoylation, the interaction of RP2 with Arl3 and the C-terminal domain of RP2 were not essential.

### RP2 and Arl3 regulate vesicle traffic

As RP2 is a GAP for Arl3 (9), we tested the hypothesis that a constitutively active conformational mimic of Arl3-GTP (Arl3-Q71L) would alter RP2 localization. RP2-GFP alone localized mainly to the plasma membrane, as described previously (4,5,7), whereas Arl3-T31N (an Arl3-GDP mimic) and Arl3-Q71L were diffusely distributed in the cytoplasm and nucleus (Fig. 3A). Co-expression of RP2 and Arl3-Q71L resulted in a dramatic translocation of both proteins (Fig. 3C). RP2 recruited Arl3-Q71L to the plasma membrane and both proteins now decorated multiple intracellular vesicles (Fig. 3C). In contrast, the cellular localization of RP2 and Arl3 were unchanged with co-expression of RP2 and Arl3-T31N (Fig. 3B) or RP2 and Arl3 (data not shown). Live cell imaging of RP2 co-expressed with Arl3-Q71L revealed that RP2 decorates intracellular vesicles that move predominantly away from the perinuclear region towards the plasma membrane, implying a role for RP2 in Golgi vesicle loading or transport.

To test this hypothesis, ER to plasma membrane transport of ts045 VSVG-GFP was analysed in RP2 depleted cells and cells transfected with Arl3 mutants. The export of proteins from the ER to the Golgi was intact (Supplementary Material, Fig. S6), suggesting that RP2 and Arl3 may be involved in post-Golgi vesicle transport. Post-Golgi transport was analysed and quantified by measuring the distance of VSVG-GFP positive vesicles from the Golgi complex. Cells transfected with Arl3-Q71L had

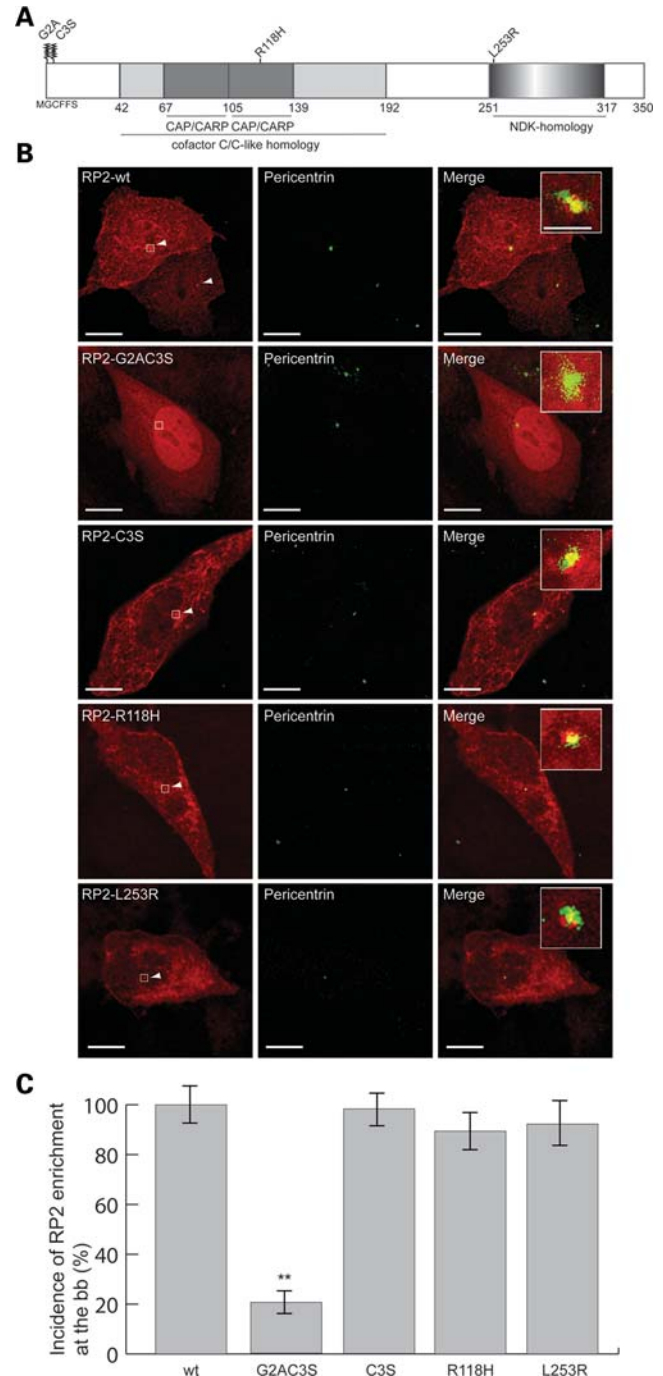


**Figure 2.** RP2 targeting to the ciliary base is dependent on myristoylation. (A) Domain structure of RP2. The RP2 protein has a dual acylation motif for myristoylation and palmitoylation at the N-terminus, followed by a TBCC homology domain. At the C-terminus RP2 shares structural homology with a nucleoside diphosphate kinase (NDK) domain. (B) IMCD3 cells were transfected with wild-type RP2 and mutant constructs, as indicated, to determine which domain regulates RP2 targeting to the basal body. The mutants targeted the two acylation sites, as well as patient mutations R118H and L253R highlighted in (A). Loss of the myristoylation motif caused mislocalization of RP2. RP2 (red) and pericentrin (green). Arrowheads show localization to the basal body. Scale bar 10  $\mu$ m. Insets show higher magnification of boxed area, scale bar 0.5  $\mu$ m. (C) Quantification of basal body localization of wild-type and mutant RP2. Experiments were performed in triplicate. Values are means  $\pm$  SEM,  $n = 100$  cells,  $**P \leq 0.01$ .

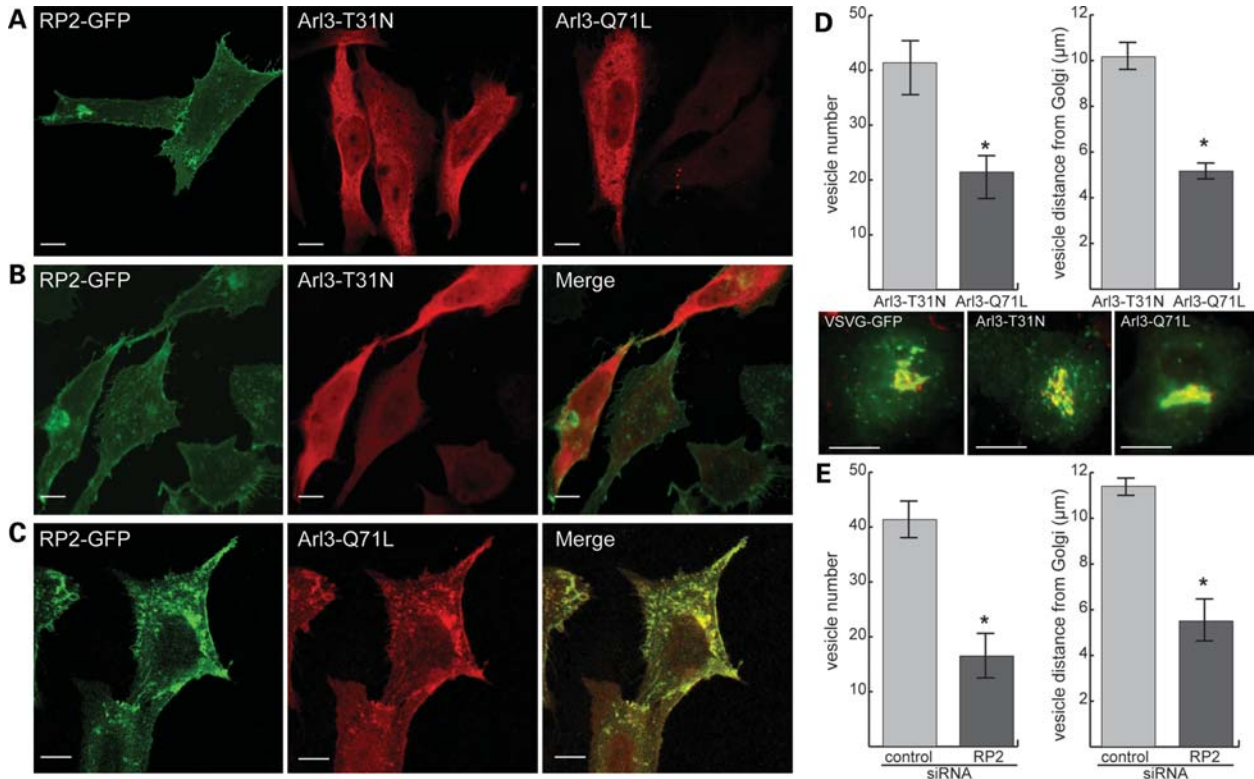


**Figure 3.** RP2 and Arl3 regulate vesicle traffic. (A) RP2-GFP (green) localized predominantly to the plasma membrane of CHO cells, whereas both myc-Arl3-T31N (red) and myc-Arl3-Q71L (red) were localized throughout the cytoplasm. Scale bar 10  $\mu\text{m}$ . (B) Co-expression of RP2 (green) with the Arl3-T31N (red) did not affect localization of either protein. Scale bar 10  $\mu\text{m}$ . (C) Co-expression of RP2 and Arl3-Q71L resulted in re-localization of both proteins with extensive co-localization decorating intracellular vesicles and plasma membrane. Scale bar 10  $\mu\text{m}$ . (D) Quantification of vesicle traffic in ARPE19 cells transfected with VSVG-GFP (green) and Arl3-Q71L or Arl3-T31N and stained for the Golgi marker GM130 (red). Following 12 h incubation at 40°C cells were shifted to 32°C for 40 min. Vesicle number and vesicle distance from the Golgi was decreased in cells transfected with Arl3-Q71L compared with Arl3-T31N. Values are means  $\pm$  SEM,  $n = 500$  vesicles,  $*P \leq 0.05$ . Representative images of cells co-transfected with VSVG-GFP only, Arl3-T31N or Arl3-Q71L and VSVG-GFP are shown. Scale bar 10  $\mu\text{m}$ . (E) Quantification of vesicle traffic in ARPE19 cells transfected with control or RP2 siRNA. The average number of VSVG-GFP vesicles in RP2 depleted cells and their distance from the Golgi after incubation at 32°C for 40 min was decreased compared to control siRNA. Values are means  $\pm$  SEM,  $n = 300$  vesicles,  $*P \leq 0.05$ .

a significant decrease in vesicle number and these vesicles did not traffic as efficiently away from the Golgi compared with cells transfected with Arl3-T31N (Fig. 3D), which was the same as control VSVG-GFP alone (Fig. 3D and data not shown). Co-expression of RP2-GFP with the Arl3 mutants did not alter the Arl3-Q71L effect (data not shown). As RP2 is a negative regulator of Arl3, we predicted that depletion of RP2 by siRNA should phenocopy the effect of Arl3-Q71L. RP2 siRNA resulted in a significant decrease in average vesicle number and vesicle distance from the Golgi (Fig. 3E), imitating the effect of Arl3-Q71L as predicted. These data suggest that RP2 and Arl3 are both involved in post-Golgi vesicle traffic, and that RP2 regulates this process by controlling Arl3 activity.

#### Knock-down of RP2 affects Golgi cohesion and docking of cilia proteins

To probe the mechanisms of this effect on post-Golgi traffic, we examined RP2 localization and the effect of its depletion on Golgi function. In addition to the localization of RP2 at the photoreceptor cilia base, immunoelectron microscopy of mouse retinal sections revealed RP2 staining at the periciliary ridge and the Golgi complex (Fig. 4A and B). The periciliary

ridge, Golgi complex and basal body function in close association with each other to control and regulate export from the inner to the outer segment of photoreceptor cells (20,21). The localization of RP2 to these structures supports a role for RP2 in pericentriolar vesicle trafficking and IFT.

Kif3a, a component of IFT, is a subunit of the heterotrimeric Kinesin-2 motor which has been shown to be important in cilia maintenance and transport of proteins through the connecting cilium in photoreceptors (29). Furthermore, down regulation of Kif3a and Arl3 in HeLa cells causes fragmentation of the Golgi (30,31). Therefore, we investigated the effect of RP2 knock-down on Golgi morphology. The degree of Golgi dispersal was determined as described previously (32). Briefly, Golgi fragmentation was blindly scored according to whether the Golgi staining was predominantly punctate and dispersed throughout the cytoplasm or compact and tight in reference to the basal body marker pericentrin. Similar to Kif3a and Arl3 depletion, loss of RP2 led to fragmentation of the *cis*, *cis*-medial and *trans* Golgi network (TGN; Fig. 4C and D). The TGN is a major site in protein biosynthetic pathways for the sorting of different cargo molecules and directing them to distinct acceptor compartments (33). Fragmentation of the TGN could lead to missorting and

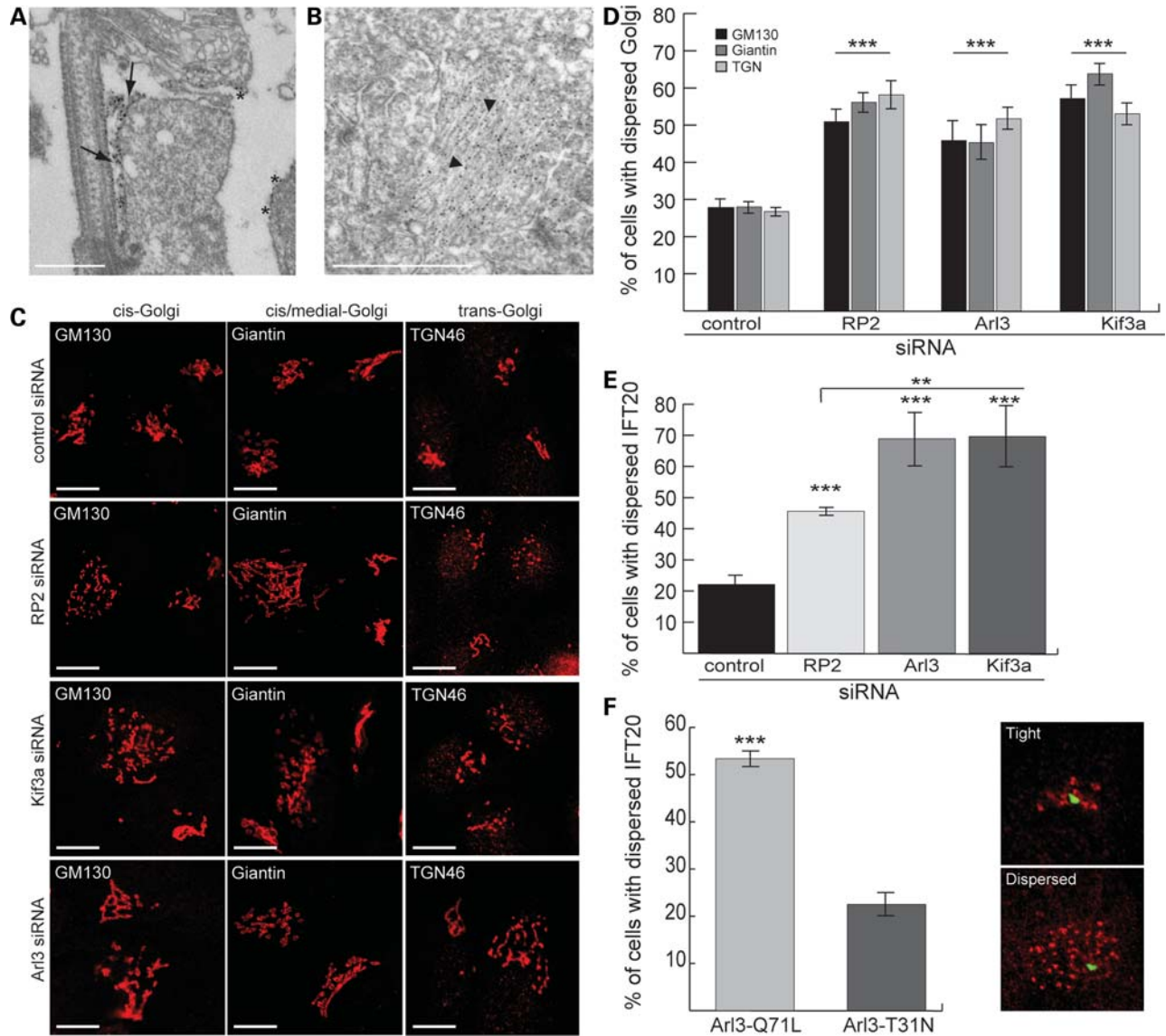


**Figure 4.** RP2 and Arl3 are necessary for Golgi cohesion and pericentriolar localization of IFT20. (A) Immunoelectron microscopy shows that RP2 localized to the periciliary ridge in murine photoreceptors, a key docking site for vesicles destined for the outer segment of the photoreceptor (see arrow). RP2 was also observed on the plasma membrane of the photoreceptor (as shown by the asterisk) and (B) the Golgi apparatus (arrowheads) in the murine retina. (C) ARPE19 cells treated with siRNA for RP2, Arl3, Kif3a and a non-targeting control were stained with antibodies to the *cis*, *cis*-medial and *trans* Golgi components GM130, Giantin and TGN46, respectively to determine disruption to any specific part of the complex. Scale bar 10  $\mu$ m. (D) Golgi dispersal was quantified for RP2, Arl3 and Kif3a siRNA and compared with control siRNA. All parts of the Golgi complex were equally dispersed in the Kif3a, RP2 and Arl3 knockdown cells. Values are means  $\pm$  SEM,  $n = 250$  cells,  $***P < 0.001$ . ARPE19 cells treated with siRNA (E) or transfected with Arl3 (F), as indicated were stained for pericentrin (green) and IFT20 (red) and categorized for 'tight' (normal pattern around the centrosome) or 'dispersed' (fragmented appearance) staining. Representative examples of the categories are shown next to the graph. Scale bar 5  $\mu$ m. Values are means  $\pm$  SEM,  $n = 250$  cells,  $***P \leq 0.001$ ,  $**P \leq 0.01$ .

impaired loading of cargo onto vesicles, thereby depriving cellular organelles, such as the photoreceptor cilium, of vital proteins.

To further investigate this hypothesis we examined whether loss of RP2 affected the localization of IFT20, a protein known to shuttle between the Golgi and cilium. IFT20 is a component of the classic IFT machinery and localizes to the cilium and peri-basal body pool, as well as to the Golgi complex (34). ARPE19 cells were depleted of Arl3, Kif3a or RP2 and stained for IFT20. The majority of IFT20 in cells treated with control siRNA was associated with the Golgi

complex and localized tightly around the basal body, in accordance with previously published data (34). However,  $\sim 20\%$  of cells showed a dispersed IFT20 staining pattern with the control siRNA, which is likely to correlate with Golgi complex re-organization at different stages of the cell cycle. Depletion of RP2, or expression of Arl3-Q71L, caused a significant, 2-fold increase in the incidence of dispersed IFT20 (Fig. 4E and F). Cells depleted of Kif3a and Arl3 showed a 3-fold increase in dispersed, and therefore, mis-localized IFT20, compared with control (Fig. 4F). These data show that loss of RP2 and dysregulated Arl3 disrupts Golgi

complex cohesion, thereby affecting the location and trafficking of cilia proteins, such as IFT20.

## DISCUSSION

Patients with RP2 mutations appear to only have a retinal pathology without any other organ involvement. In this study, we show RP2 localization to the ciliary apparatus, specifically to the cilium-associated centriole and the basal body in cultured cells (ARPE19) and murine photoreceptor cells.

RP2 contains a homology domain of 151 amino acids (30% identity) to TBCC. The majority of RP2 missense mutations are found in the TBCC-like domain at residues conserved with TBCC or TBCCD1. The identification of a homologue of TBCC and RP2 in trypanosomes (TbRP2), which localized to the mature basal body of the flagellum, led to the proposal that TbRP2 recruits and monitors the quality of carboxyl-tyrosinated  $\alpha$ -tubulin prior to cilia assembly. Ablation of TbRP2 led to abnormally short flagella and loss of carboxyl-tyrosinated  $\alpha$ -tubulin staining (YL 1/2) at the basal body (25). This is in contrast to findings in this study, as the number of cells expressing cilia, as well as cilia morphology and length, was unaffected by RP2 knock-down. Furthermore, RP2 knock-down did not affect localization of YL 1/2. This can be explained by the striking structural differences between the RP2 protein in humans and TbRP2 in *Trypanosomes*. For example, TbRP2 lacks the N-terminal dual acylation motif and C-terminal NDK domain, both of which are likely to contribute to RP2 function as patient mutations compromise these motifs. Conversely, RP2 does not have the FOP N-terminal dimerization domain present in TbRP2. These differences might help explain why the RP2 phenotype is restricted to the retina, despite the ubiquitous expression of the protein and importance of cilia in other organs.

RP2 myristoylation is essential for RP2 localization at the basal body. Myristoylation and palmitoylation of RP2 have previously been shown to be necessary to target the protein to the cytoplasmic face of the plasma membrane in cultured cells (4) and in cells throughout the retina (5). Pathogenic mutations of the N-terminus of RP2 have been shown to prevent plasma membrane localization of RP2 (4,6,7), illustrating that post-translational modifications are vital for correct localization and function of the protein. Several studies in protozoa have shown the importance of acylation for correct targeting of proteins to flagella (35,36). Furthermore, proteins with myristoylation motifs are enriched in the *Chlamydomonas* flagellar proteome (37) and a recent study (38) confirmed that myristoylation is important for targeting of ciliary proteins in mammals. This study provides additional evidence for the importance of protein myristoylation for correct localization of a basal body protein in mammalian cells.

RP2 is a GAP for Arl3 (9) and co-expression of Arl3-Q71L and RP2 altered the localization of both proteins. RP2 recruits Arl3-Q71L to the plasma membrane and both proteins decorate intracellular vesicles. Many small GTPases have a dynamic membrane association regulated by acylated N-termini exposure following GTP binding. The N-terminal

acylation status of Arl3 is controversial and there is no direct evidence for the acylation of mammalian Arl3 (39). However, *Drosophila* Arl3 is acetylated, not acylated, and associates with both intracellular vesicles and microtubules (40). The direct membrane association of Arl3-Q71L was only revealed by co-expression with RP2-GFP, but not when expressing Arl3-Q71L alone (either myc-Arl3 or Arl3-vsv; data not shown). Therefore, expression of the constitutively active Arl3 with its GAP, RP2, sequesters and concentrates both proteins at a normally transient interaction site on internal vesicles. These data suggest both Arl3 and RP2 can bind vesicles and may regulate vesicle traffic. The Arl3-GDP mimic, Arl3-T31N, behaved the same as wild-type Arl3 in all of the above assays (data not shown), suggesting that the majority of Arl3 in cells is in a GDP-bound state (41) or that Arl3-T31N is a poor GDP conformational mimic.

In addition to the basal body, RP2 localizes to the periciliary ridge and the Golgi complex. These structures are known to function in association with each other to control import and export in photoreceptor cells (20,21). Therefore, localization of RP2 to these specific structures supports a role of RP2 in pericentriolar vesicle trafficking and IFT. Kif3a is an important component of IFT and it has been hypothesized that Kif3a plays a role in membrane organization of the Golgi complex, linking motor activity and organelle morphology (30). Depletion of Kif3a leads to significant dispersal of the Golgi complex and the observed changes in Golgi morphology following RP2 knock-down implicate a potential function of RP2 in Golgi cohesion. RP2 may act in a similar pathway as Kif3a, mediating vesicle trafficking as well as maintaining Golgi structure. This hypothesis was further confirmed when depletion of RP2 caused dispersal of IFT20 from the peri-basal body pool.

In conclusion, the presence of RP2 at the Golgi complex, base of the cilium (basal body and cilium associated centriole) and periciliary ridge indicate that RP2 is ideally localized to couple the directed movement of proteins destined for the ciliary membrane through the endomembrane system to the base of the cilium and into the cilium itself. RP2 could associate with these vesicles in the Golgi complex via N-terminal acylation. After delivery of vesicles to the base of the cilium, RP2 may also function as a docking signal for these vesicles, allowing specific unloading of the cargo at the ciliary base. The conservation of centriolar association and function in TBCC-like proteins, from ASQ2 and TbRP2 to RP2, suggests that the TBCC domain may be important for centriolar association. A likely role for this domain is to act as a GAP for members of the Arl family of small GTPases. Therefore, the orchestration of Arl function by TBCC-like proteins and unidentified GEFs will be essential for different aspects of centriolar function.

We have shown that Arl3 plays a vital role in vesicle traffic from the Golgi to the cilium, and that negative regulation of Arl3 by RP2 is important for vesicle trafficking from the Golgi to the base of the cilium. Depletion of RP2 leads to milder vesicle organization defects than depletion of Kif3a and Arl3, therefore RP2 mutations may not affect all cilia to the same extent and a phenotype may only be revealed at the sites where demand on trafficking is greatest. The outer segment of photoreceptors has a high metabolic turnover

rate and alterations in efficiency of protein delivery to the basal body could result in progressive degeneration of the photoreceptor cilium and subsequent cell death. We propose that the fragmentation of the Golgi caused by loss of RP2 and subsequent mislocalization of important cilia proteins, such as IFT20, have a long-term effect on maintenance, stability and metabolism of the cilium photoreceptors.

## MATERIALS AND METHODS

### Cell culture and transfections

Human retina pigment epithelial cells (ARPE19) and Chinese hamster ovary (CHO) cells and murine inner medullary collecting duct 3 (IMCD3) cells were grown in Dulbecco's modified Eagle's medium (DMEM)/F12 (Invitrogen, Paisley, UK). Serum-rich medium contained additionally 10% (v/v) fetal bovine serum (FBS). Cell cultures were not treated with antibiotics. For maintenance, cells were passaged every 3–4 days or when they were ~90% confluent. For immunofluorescent staining, cells were cultured in 8-well chamber slides (VWR, Lutterworth, UK). Cells for western blotting were plated into 24-well plates (Nunc, Fisher Scientific, UK). Transfections of plasmids were performed using Lipofectamine and Lipofectamine Plus reagent according to the manufacturer's instructions (Invitrogen). Per well, 100 ng of the eukaryotic expression vector pBKCMV containing full-length wild-type RP2 and the RP2 mutants (RP2 C3S-pBKCMV, RP2 G2A-pBKCMV, RP2 G2AC3S-pBKCMV, RP2 R118H-pBKCMV and RP2L253R-pBKCMV) were transfected into IMCD3 cells. Generation of these RP2 mutants using site-directed mutagenesis has been described elsewhere (4). Wild-type human Arl3 cDNA was amplified from an IMAGE clone (# 3926032) and introduced into the pcDNA4/TO/VSV plasmid (a gift from Dr Karl Matter, UCL Institute of Ophthalmology, London, UK) using *EcoRI* and *SacII* restriction sites. The Arl3 mutants glutamine 71 to leucine (Q71L) and threonine 31 to asparagine (T31N) were created using site-directed mutagenesis (QuikChange, Qiagen, Crawley, UK) and represent the GTP- and GDP-bound conformation of the Arl3 protein, respectively. CHO cells were transfected with 10 ng RP2-GFP and 90 ng of either Arl3-Q71L-myc or Arl3-T31N-myc using the Lipofectamine transfection reagents according to manufacturer's instructions. To create IMCD3 cells stably expressing human wild-type or mutant RP2 pBKCMV plasmids, cells were transfected with 1 µg of plasmid using Lipofectamine and Lipofectamine Plus reagents. Cells were subsequently cultured in selection medium (DMEM/F12, 10% FBS, 100 µg/ml penicillin/streptomycin, 0.6 mg/ml G418). RP2 protein expression was determined by western blotting with crude sheep anti-RP2 antibody (1:2000), which recognizes human, but not mouse RP2 protein.

### VSVG-GFP trafficking assay

ARPE19 cells were seeded in 8-well chamber slides and transfected with 100 ng GFP tagged vesicular stomatitis virus glycoprotein (VSVG-GFP, gift from Dr Ben Nichols, LMB Cambridge, UK) per well as previously described. One hour post-transfection, cells were moved from 37–40°C for

12 h. Cells were then shifted to 32°C for 40 min and subsequently fixed in 4% (v/v) paraformaldehyde as described in what follows. Measurements of vesicle distance from the Golgi complex and counts of vesicle numbers were performed using a Nikon Eclipse 80i microscope and Nikon NIS-Elements software (Basic Research, Version 2.2, Nikon).

### Antibodies

Production and characterization of affinity-purified sheep polyclonal RP2 antisera S974 has been described previously (4,7). The following antibodies were used as centrosomal markers: rabbit anti-γ-tubulin (1:1000, Abcam, Cambridge, UK), rabbit anti-ninein (1:2000, was a gift from Dr J.B. Rattner, Department of Cell Biology and Anatomy, University of Calgary, Canada) mouse anti-centrin-3 (1:2) (26) and rabbit anti-pericentrin (1:2000, Abcam). Mouse anti-acetylated α-tubulin (1:1000, Sigma-Aldrich, Dorset, UK) was used as a marker for cilia. The rabbit anti-Kif3a antibody (1:2000) was from Abcam. The antibody against rat anti-detyrosinated tubulin YL1/2 (1:1000) was from AbD Serotec (Kidlington, UK). The rabbit anti-Arl3 antibody was a gift from Dr N.J. Cowan (New York University, USA). The guinea-pig anti-IFT20 (1:200) antibody was a gift from Dr J. C. Besharse (Cell Biology Department, Medical College of Wisconsin, Milwaukee, USA). The following antibodies were used as Golgi markers: GM130 (1:100, Clone 35, BD Biosciences, Oxford, UK), TGN-46 (1:1000, Abcam), Giantin (1:500, Abcam). The rabbit anti-Calnexin antibody was obtained from Abcam (1:500).

### Immunocytochemistry

For immunocytochemistry (ICC), cells were washed twice in PBS and either fixed in 100% ice-cold methanol for 2 min or 4% (v/v) paraformaldehyde for 10 min. Cells were permeabilized with 0.2% (v/v) Triton X-100 in PBS for 10 min and subsequently incubated for 1 h in blocking buffer [3% (w/v) bovine serum albumin (BSA), 10% (v/v) normal donkey serum in PBS] to avoid non-specific antibody binding. Following block cells were incubated for 1 h with primary antibodies at the appropriate titre. After washing with PBS cells were then incubated with fluorescent labelled (Cyanine2 or Cyanine3) secondary antibodies (1:100, Stratech, Newmarket, Suffolk, UK) for 1 h in 3% (w/v) BSA in PBS. Following several washes with PBS cells were incubated for 5 min with 4',6-diamidino-2-phenylindole (DAPI, 1:5000, Sigma-Aldrich) in PBS to stain the nuclei. Confocal images were obtained using the LSM510 microscope (Carl Zeiss MicroImaging) and analysed using the LSM Image Browser software (Carl Zeiss MicroImaging). For live imaging cells were seeded into 35 mm dishes with a central glass coverslip (MatTek, Ashland, USA) at a density of 200 000 cells/dish and transfected as previously described. Twenty hours after transfection the cells were observed using a Zeiss Axiovert M100 microscope and Improvison software. Images were captured every 15 s for a duration of 10 min.

### Immunohistochemistry and retina cryosections

Eyes of adult wild-type C57Bl6 mice were cryofixed in melting isopentane and cryosectioned as described elsewhere (42). Cryosections were placed on poly-L-lysine-precoated coverslips and incubated subsequently with 0.01% Tween 20 in PBS. After PBS washing sections were incubated with blocking solution (0.5% cold-water fish gelatine plus 0.1% ovalbumine in PBS) followed by overnight incubation with primary antibodies diluted in blocking solution at 4°C. Washed cryosections were incubated with secondary antibodies conjugated to Alexa dyes in PBS with DAPI (Sigma-Aldrich). After washing with PBS sections were mounted in Mowiol 4.88 (Hoechst, Frankfurt, Germany) and analysed in a Leica DMRB microscope (Leica, Wetzlar, Germany). Images were obtained with a charge-coupled device camera (ORCA ER, Hamamatsu, Herrsching, Germany) and processed with Adobe Photoshop CS (Adobe Systems, San Jose, USA).

### Immunoelectron microscopy

Immuno-EM was carried out as described previously (21). Eyes of mature mice (C57Bl6) were fixed in 4% buffered paraformaldehyde, infiltrated with 30% buffered sucrose and cracked by cycles of freezing in liquid nitrogen and thawing at 37°C. Fifty micrometer thick vibratome sections were incubated with affinity purified RP2 antibody and a biotinylated anti-sheep secondary antibody (Vector Laboratories) and visualized by a Vectastain ABC-Kit (Vector Laboratories). After silver enhancement, post-fixation, and dehydration, specimens were embedded in araldite. Ultra-thin sections were analysed in a Tecnai 12 BioTwin transmission electron microscope (FEI, Eindhoven, The Netherlands).

### RNA interference

For RNA interference studies ARPE19 cells were plated either plated into 8-well chamber slides (VWR) for ICC or 24-well plates (Nunc) for analysis of protein knockdown. A pool of four small interfering RNAs (siRNA) for RP2, Arl3 and Kif3a in addition to a non-targeting control siRNA were obtained from Dharmacon (ON-TARGET plus siRNA reagents, Chicago, USA). The sequences of these siRNAs (sense strands) are as follows: non-targeting control siRNA: 5'-UAGCGACUAAACACAUCAA-3'; RP2 siRNA: 5'-GACAAUACAUGGAGUAACAUU-3', 5'-GAAGAGCAGCGAUGAAUCAUU-3', 5'-UGAAACAGUAGGUCGCUUAUU-3', 5'-GGUAUUUUUGCUGGUGAUUU-3'; Arl3 siRNA: 5'-GUCAGGAACUAGCGAAUUUU-3', 5'-GUGCUCUAUCUUGCUAAUAUU-3', 5'-GAAGGACUGAACCUGCAUAUU-3', 5'-GAUAAACGGCCUCUGUAAAUUU-3'; Kif3a siRNA: 5'-CAACUAAUAUGAACGAACA-3'; 5'-UAUCGUAACUCUAAACUGA-3', 5'-GGACCUUCUCACGUGUAU-3'; 5'-GGCCAGCAGAUUACAAUUA-3'. For western blotting of RP2, Arl3 or Kif3a protein expression following siRNA treatment crude sheep anti-RP2 antibody (1:2000), rabbit anti-Arl3 antibody (1:2000) or rabbit anti-Kif3a antibody (1:2000) were used, respectively. Additionally, lysates were blotted with a mouse anti-glyceraldehyde-3-phosphate dehydrogenase

(GAPDH) antibody (1:40 000, Sigma-Aldrich) to ensure equal loading of samples. Secondary antibodies used were horseradish peroxidase (HRP) conjugated goat anti-sheep, donkey anti-rabbit or goat anti-mouse antibodies (Strattech). Blots were developed using the enhanced chemiluminescence (ECL) western blotting detection system (GE Healthcare, Chalfont St Giles, UK).

### SUPPLEMENTARY MATERIAL

Supplementary Material is available at *HMG* online.

### ACKNOWLEDGEMENTS

We are grateful to N. Cowan, J. Besharse and J. Rattner for the gift of the antibodies; B. Nichols and K. Matter for plasmids. We also thank E. Sehn for technical assistance in immunotEM preparations and analysis.

*Conflict of Interest statement.* None declared.

### FUNDING

This work was supported by Fight for Sight (1621 to M.E.C. and A.J.H.), the British Retinitis Pigmentosa Society (GR533 to M.E.C. and A.J.H.), the FAUN foundation (to U.W.) and Research Funds University of Mainz (to K.N.W.).

### REFERENCES

- Schwahn, U., Lenzer, S., Dong, J., Feil, S., Hinzmann, B., van Duijnhoven, G., Kirschner, R., Hemberger, M., Bergen, A., Rosenberg, T. *et al.* (1998) Positional cloning of the gene for X-linked retinitis pigmentosa 2. *Nat. Genet.*, **19**, 327–332.
- Hardcastle, A.J., Thiselton, D., van Maldergem, L., Saha, B., Jay, M., Plant, C., Taylor, R., Bird, A. and Bhattacharya, S.S. (1999) Mutations in the RP2 gene cause disease in 10% of families with familial X-linked retinitis pigmentosa assessed in this study. *Am. Hum. J. Genet.*, **64**, 1210–1215.
- Miano, M., Testa, F., Filippini, F., Trujillo, M., Conte, I., Lanzara, C., Millan, J., De Bernardo, C., Grammatico, B., Mangino, M. *et al.* (2001) Identification of novel RP2 mutations in a subset of X-linked retinitis pigmentosa families and prediction of new domains. *Hum. Mutat.*, **18**, 109–119.
- Chapple, J.P., Hardcastle, A.J., Grayson, C., Spackman, L.A., Willison, K.R. and Cheetham, M.E. (2000) Mutations in the N-terminus of the X-linked retinitis pigmentosa protein RP2 interfere with the normal targeting of the protein to the plasma membrane. *Hum. Mol. Genet.*, **9**, 1919–1926.
- Grayson, C., Bartolini, F., Chapple, J.P., Willison, K.R., Bhamidipati, A., Lewis, S.A., Luthert, P.J., Hardcastle, A.J., Cowan, N.J. and Cheetham, M.E. (2002) Localization in the human retina of the X-linked retinitis pigmentosa protein RP2, its homologue cofactor C and the RP2 interacting protein Arl3. *Hum. Mol. Genet.*, **11**, 3065–3074.
- Schwahn, U., Paland, N., Techritz, S., Lenzer, S. and Berger, W. (2001) Mutations in the X-linked RP2 gene cause intracellular misrouting and loss of the protein. *Hum. Mol. Genet.*, **10**, 1177–1183.
- Chapple, J.P., Hardcastle, A.J., Grayson, C., Willison, K.R. and Cheetham, M.E. (2002) Delineation of the plasma membrane targeting domain of the X-linked retinitis pigmentosa protein RP2. *Invest. Ophthalmol. Vis. Sci.*, **43**, 2015–2020.
- Bartolini, F., Bhamidipati, A., Thomas, S., Schwahn, U., Lewis, S.A. and Cowan, N.J. (2002) Functional overlap between retinitis pigmentosa 2 protein and the tubulin-specific chaperone cofactor c. *J. Biol. Chem.*, **277**, 14629–14634.

9. Veltel, S., Gasper, R., Eisenacher, E. and Wittinghofer, A. (2008) The retinitis pigmentosa 2 gene product is a GTPase-activating protein for Arf-like 3. *Nat. Struct. Mol. Biol.*, **15**, 373–380.
10. Schrick, J., Vogel, P., Abuin, A., Hampton, B. and Rice, D. (2006) ADP-ribosylation factor-like 3 is involved in kidney and photoreceptor development. *Am. J. Pathol.*, **168**, 1288–1298.
11. Quarmby, L.M. and Parker, J.D.K. (2005) Cilia and the cell cycle? *J. Cell Biol.*, **169**, 707–710.
12. Davenport, J.R. and Yoder, B.K. (2005) An incredible decade for the primary cilium: a look at a once-forgotten organelle. *Am. J. Physiol. Renal Physiol.*, **289**, 1159–1169.
13. Hildebrandt, F. and Otto, E. (2005) Cilia and centrosomes: a unifying pathogenic concept for cystic kidney disease? *Nat. Rev. Genet.*, **6**, 928–940.
14. Christensen, S.T., Pedersen, L.B., Schneider, L. and Satir, P. (2007) Sensory cilia and integration of signal transduction in human health and disease. *Traffic*, **8**, 97–109.
15. Fliegauf, M., Benzing, T. and Omran, H. (2007) When cilia go bad: cilia defects and ciliopathies. *Nat. Rev. Mol. Cell Biol.*, **8**, 880–893.
16. Adams, N., Awadein, A. and Toma, H. (2007) The retinal ciliopathies. *Ophthalmic Genet.*, **28**, 113–125.
17. Marszalek, J.R., Liu, X., Roberts, E.A., Chui, D., Marth, J.D., Williams, D.S. and Goldstein, L.S.B. (2000) Genetic evidence for selective transport of opsin and arrestin by kinesin-II in mammalian photoreceptors. *Cell*, **102**, 175–187.
18. Jimeno, D., Feiner, L., Lillo, C., Teofilo, K., Goldstein, L.S.B., Pierce, E.A. and Williams, D.S. (2006) Analysis of kinesin-2 function in photoreceptor cells using synchronous cre-loxP knockout of Kif3a with RHO-Cre. *Invest. Ophthalmol. Vis. Sci.*, **47**, 5039–5046.
19. Pazour, G.J., Baker, S.A., Deane, J.A., Cole, D.G., Dickert, B.L., Rosenbaum, J.L., Witman, G.B. and Besharse, J.C. (2002) The intraflagellar transport protein, IFT88, is essential for vertebrate photoreceptor assembly and maintenance. *J. Cell Biol.*, **157**, 103–114.
20. Roepman, R. and Wolfrum, U. (2007) Protein networks and complexes in photoreceptor cilia. *Subcell. Biochem.*, **43**, 209–235.
21. Maerker, T., van Wijk, E., Overlack, N., Kersten, F.F.J., McGee, J., Goldmann, T., Sehn, E., Roepman, R., Walsh, E.J., Kremer, H. *et al.* (2008) A novel Usher protein network at the periciliary reloading point between molecular transport machineries in vertebrate photoreceptor cells. *Hum. Mol. Genet.*, **17**, 71–86.
22. Pazour, G.J. and Rosenbaum, J.L. (2002) Intraflagellar transport and cilia-dependent diseases. *Trends Cell Biol.*, **12**, 551–555.
23. Rosenbaum, J.L. and Witman, G.B. (2002) Intraflagellar transport. *Nat. Rev. Mol. Cell Biol.*, **3**, 813–825.
24. Tian, G., Huang, Y., Rommelaere, H., Vandekerckhove, J., Ampe, C. and Cowan, N.J. (1996) Pathway leading to correctly folded  $\beta$ -tubulin. *Cell*, **86**, 287–296.
25. Stephan, A., Vaughan, S., Shaw, M., Gull, K. and McKean, P. (2007) An essential quality control mechanism at the eukaryotic basal body prior to intraflagellar transport. *Traffic*, **8**, 1323–1330.
26. Feldman, J.L. and Marshall, W.F. (2009) ASQ2 encodes a TBCC-like protein required for mother-daughter centriole linkage and mitotic spindle orientation. *Curr. Biol.*, **19**, 1238–1243.
27. Trojan, P., Giessl, A., Choe, H.W., Krauss, N., Pulvermuller, A. and Wolfrum, U. (2008) Centrin function in vertebrate photoreceptor cells. *Prog. Ret. Res.*, **28**, 237–259.
28. Evans, R.J., Hardcastle, A.J. and Cheetham, M.E. (2007) Focus on molecules: X-linked retinitis pigmentosa 2 protein, RP2. *Exp. Eye Res.*, **82**, 543–544.
29. Whitehead, J.L., Wang, S.Y., Bost-Usinger, L., Hoang, E., Frazer, K.A. and Burnside, B. (1999) Photoreceptor localization of the KIF3A and KIF3B subunits of the heterotrimeric microtubule motor Kinesin II in vertebrate retina. *Exp. Eye Res.*, **69**, 491–503.
30. Stauber, T., Simpson, J.C., Pepperkok, R. and Vernos, I. (2006) A role for Kinesin-2 in COPI-dependent recycling between the ER and the Golgi complex. *Curr. Biol.*, **16**, 2245–2251.
31. Zhou, C., Cunningham, L., Marcus, A., Li, Y. and Kahn, R.A. (2006) Arl2 and Arl3 regulate different microtubule-dependent processes. *Mol. Biol. Cell*, **17**, 2476–2487.
32. Nakagomi, S., Barsoum, M.J., Bossy-Wetzel, E., Sntterlin, C., Malhotra, V. and Lipton, S.A. (2008) A Golgi fragmentation pathway in neurodegeneration. *Neurobiol. Dis.*, **29**, 221–231.
33. De Matteis, M.A. and Luini, A. (2008) Exiting the Golgi complex. *Nat. Rev. Mol. Cell Biol.*, **9**, 273–284.
34. Folliot, J.A., Tuft, R.A., Fogarty, K.E. and Pazour, G.J. (2006) The intraflagellar transport protein IFT20 is associated with the Golgi complex and is required for cilia assembly. *Mol. Biol. Cell*, **17**, 3781–3792.
35. Godsel, L.M. and Engman, D.M. (1999) Flagellar protein localization mediated by a calcium-myristoyl/palmitoyl switch mechanism. *EMBO J.*, **18**, 2057–2065.
36. Tull, D., Vince, J.E., Callaghan, J.M., Naderer, T., Spurck, T., McFadden, G.I., Currie, G., Ferguson, K., Bacic, A. and McConville, M.J. (2004) SMP-1, a member of a new family of small myristoylated proteins in kinetoplastid parasites, is targeted to the flagellum membrane in Leishmania. *Mol. Biol. Cell*, **15**, 4775–4786.
37. Pazour, G.J., Agrin, N., Leszyk, J. and Witman, G.B. (2005) Proteomic analysis of a eukaryotic cilium. *J. Cell Biol.*, **170**, 103–113.
38. Tao, B., Bu, S., Yang, Z., Siroky, B., Kappes, J.C., Kispert, A. and Guay-Woodford, L.M. (2009) Cystin localizes to primary cilia via membrane microdomains and a targeting motif. *J. AM. Soc. Nephrol.*, **20**, 2570–2580.
39. Cavenagh, M.M., Breiner, M., Schurmann, A., Rosenwald, A.G., Terui, T., Zhang, C., Randazzo, P.A., Adams, M., Joost, H.G. and Kahn, R.A. (1994) ADP-ribosylation factor (ARF)-like 3, a new member of the ARF family of GTP-binding proteins cloned from human and rat tissues. *J. Biol. Chem.*, **269**, 18937–18942.
40. Kakihara, K., Shinmyozu, K., Kato, K., Wada, H. and Hayashi, S. (2003) Conversion of plasma membrane topology during epithelial tube connection requires Arf-like 3 small GTPase in Drosophila. *Mech. Dev.*, **125**, 325–336.
41. Linari, M., Hanzal-Bayer, M. and Becker, J. (1999) The delta subunit of rod specific cyclic GMP phosphodiesterase, PDE [delta], interacts with the Arf-like protein Arl3 in a GTP specific manner. *FEBS Lett.*, **458**, 55–59.
42. Wolfrum, U. (1991) Distribution of F-actin in the compound eye of *Calliphora erythrocephala* (Diptera, Insecta). *Cell Tiss. Res.*, **263**, 399–403.